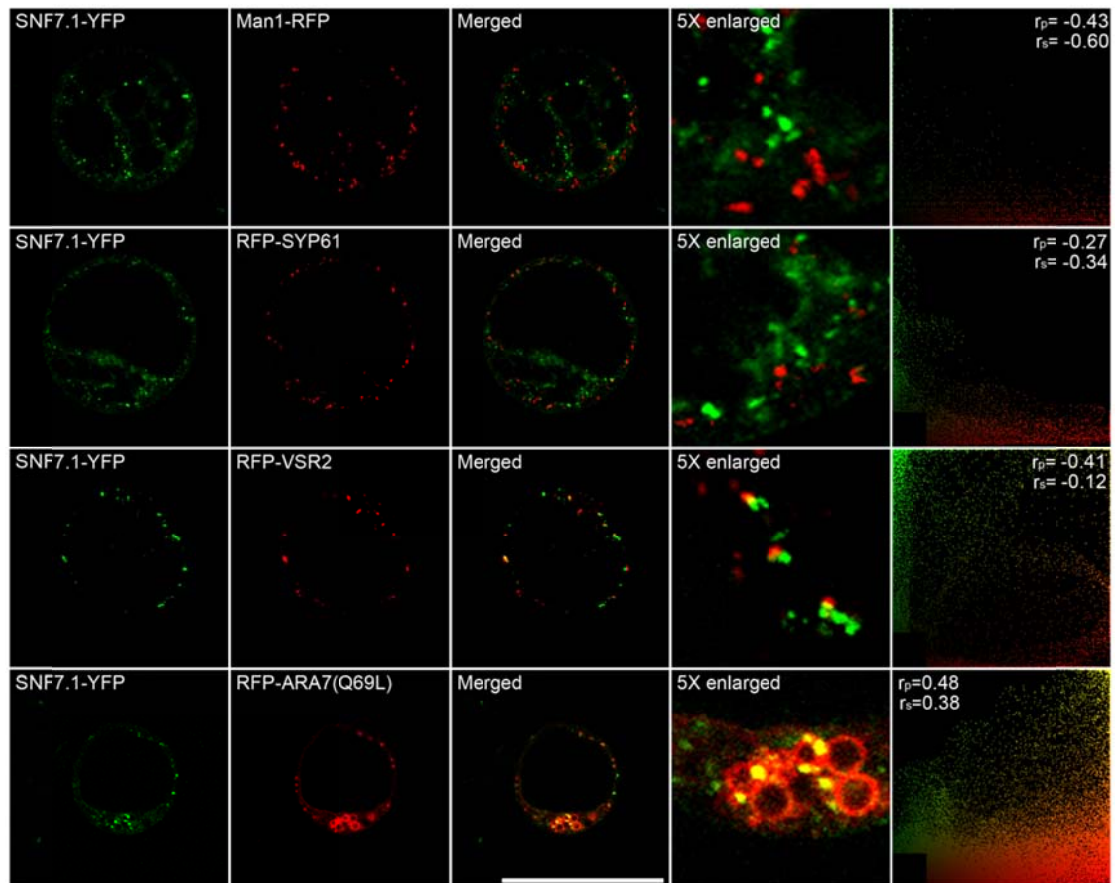


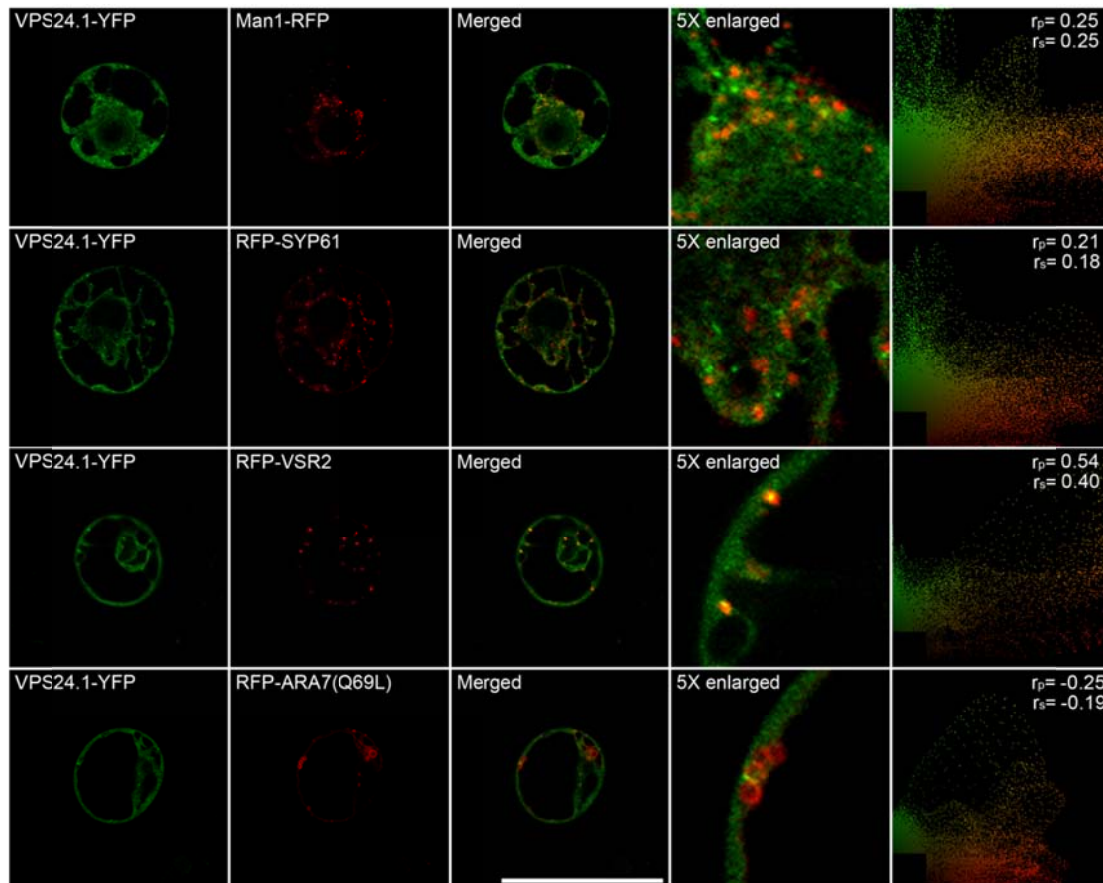
**Supplemental Figure S1.** Subcellular localizations of VPS20.1-YFP.

VPS20.1-YFP was coexpressed with different organelle markers including the Golgi marker Man1-RFP, the TGN marker RFP-SYP61, the PVC/MVB marker RFP-VSR2 and the enlarged PVC/MVB marker RFP-ARA7(Q69L) in *Arabidopsis* protoplasts. The scatterplots at the right-hand side of each row were obtained by using ImageJ program with the PSC colocalization plug-in. The corresponding Pearson or Spearman  $r$  values indicate the level of colocalization ranging from +1 for perfect colocalization to -1 for negative correlation. Scale bar = 50  $\mu\text{m}$ .



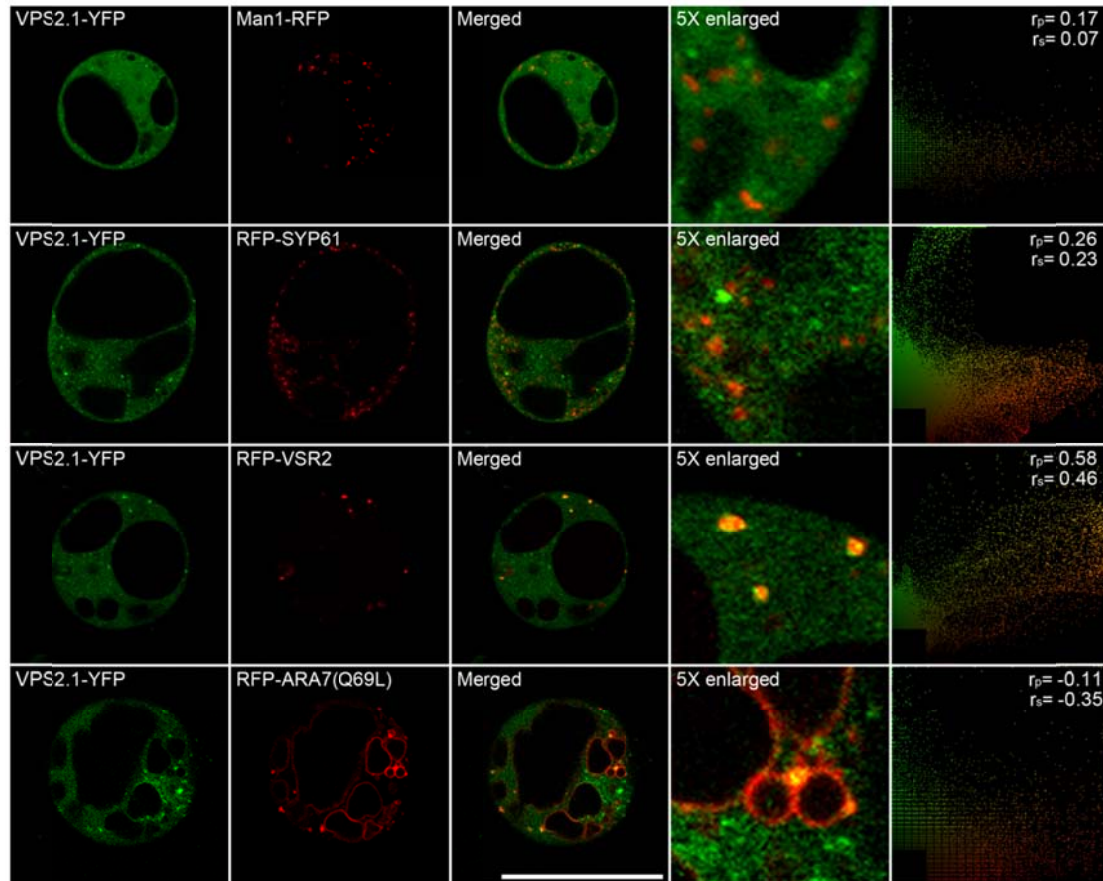
**Supplemental Figure S2.** Subcellular localizations of SNF7.1-YFP.

SNF7.1-YFP was coexpressed with different organelle markers including the Golgi marker Man1-RFP, the TGN marker RFP-SYP61, the PVC/MVB marker RFP-VSR2 and the enlarged PVC/MVB marker RFP-ARA7(Q69L) in *Arabidopsis* protoplasts. The scatterplots at the right-hand side of each row were obtained by using ImageJ program with the PSC colocalization plug-in. The corresponding Pearson or Spearman  $r$  values indicate the level of colocalization ranging from +1 for perfect colocalization to -1 for negative correlation. Scale bar = 50  $\mu\text{m}$ .



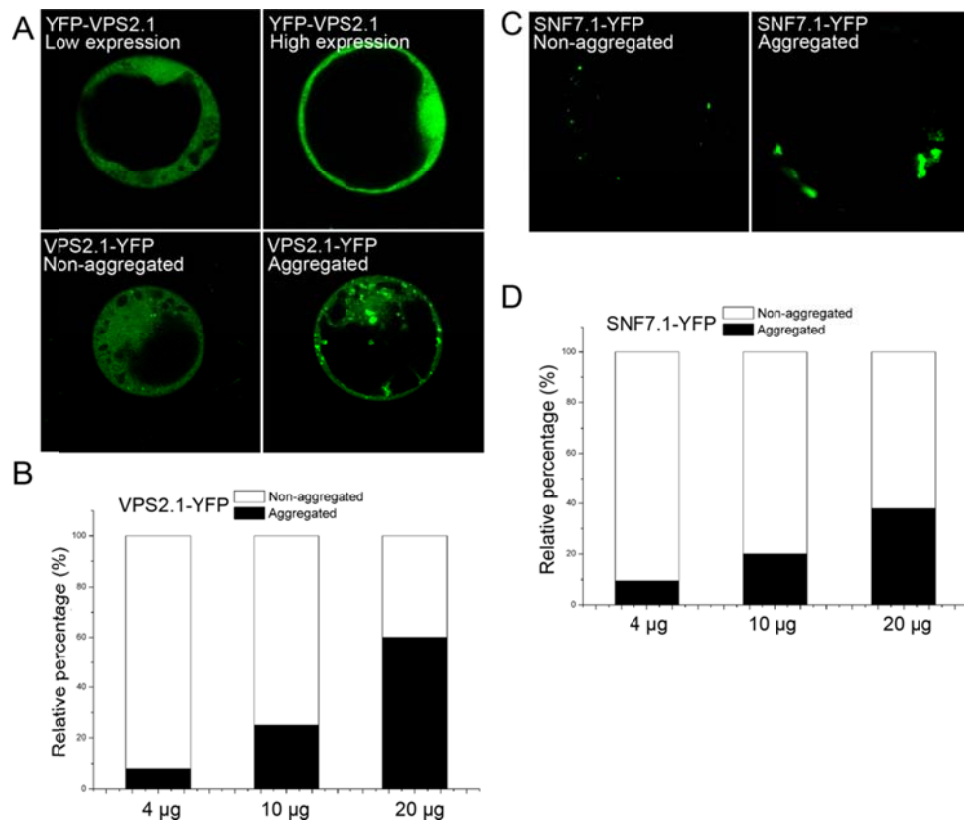
**Supplemental Figure S3.** Subcellular localizations of VPS24.1-YFP.

VPS24.1-YFP was coexpressed with different organelle markers including the Golgi marker Man1-RFP, the TGN marker RFP-SYP61, the PVC/MVB marker RFP-VSR2 and the enlarged PVC/MVB marker RFP-ARA7(Q69L) in *Arabidopsis* protoplasts. The scatterplots at the right-hand side of each row were obtained by using ImageJ program with the PSC colocalization plug-in. The corresponding Pearson or Spearman  $r$  values indicate the level of colocalization ranging from +1 for perfect colocalization to -1 for negative correlation. Scale bar = 50  $\mu$ m.



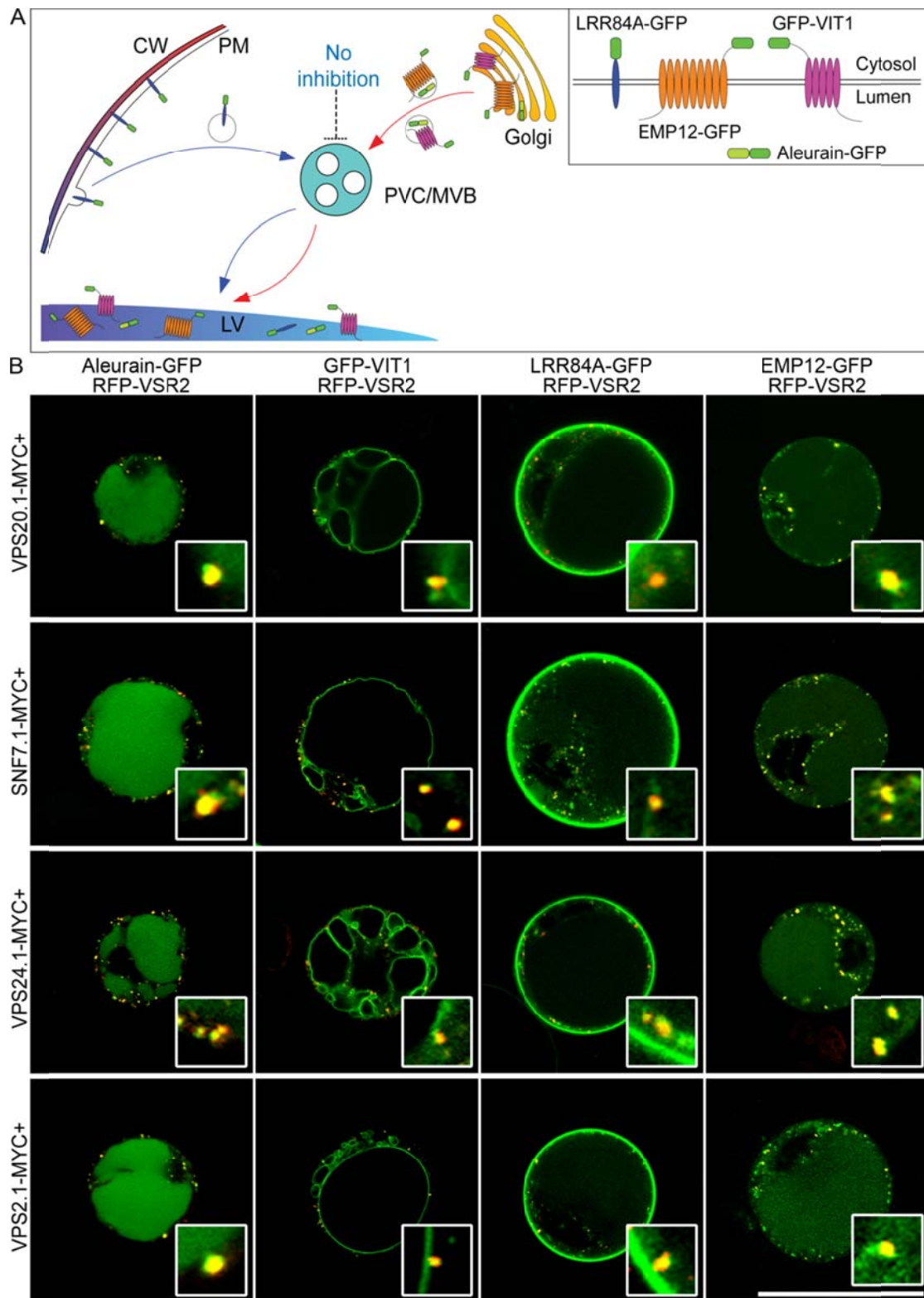
**Supplemental Figure S4.** Subcellular localizations of VPS2.1-YFP.

VPS2.1-YFP was coexpressed with different organelle markers including the Golgi marker Man1-RFP, the TGN marker RFP-SYP61, the PVC/MVB marker RFP-VSR2 and the enlarged PVC/MVB marker RFP-ARA7(Q69L) in *Arabidopsis* protoplasts. The scatterplots at the right-hand side of each row were obtained by using ImageJ program with the PSC colocalization plug-in. The corresponding Pearson or Spearman  $r$  values indicate the level of colocalization ranging from +1 for perfect colocalization to -1 for negative correlation. Scale bar = 50  $\mu\text{m}$ .



**Supplemental Figure S5.** Overexpression of SNF7.1-YFP induced aggregates.

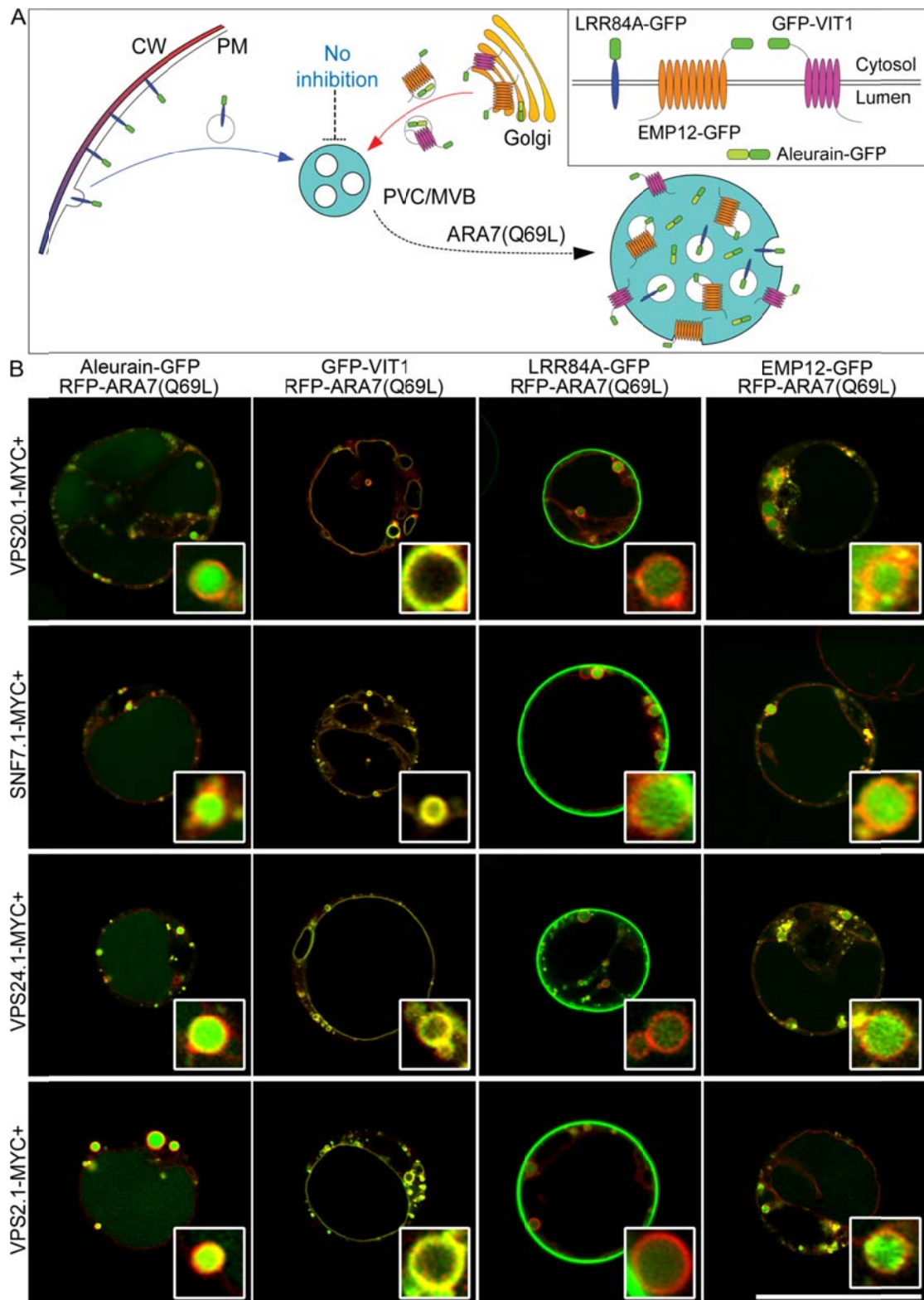
A, Representative images of protoplasts showing low expression or high expression of YFP-VPS2.1 signal and non-aggregated or aggregated VPS2.1-YFP signal. Scale bar = 50 µm. B, Percentage of protoplasts showing non-aggregated or aggregated YFP-VPS2.1 signal was correlated with the amount of plasmid DNA used in the transient expression. C, Representative images of protoplasts showing non-aggregated or aggregated SNF7.1-YFP signal. Scale bar = 50 µm. D, Percentage of protoplasts showing non-aggregated or aggregated SNF7.1-YFP signal was correlated with the amount of plasmid DNA used in the transient expression. Over 50 cells were calculated for each amount of plasmid DNA.



**Supplemental Figure S6.** Coexpression of ESCRT-III subunits did not change the expression pattern of the reporters on the LV.

A, Schematic model showing the effect of ESCRT-III coexpression on the localization of the reporters on the LV. B, Coexpression of ESCRT-III subunits with four reporters

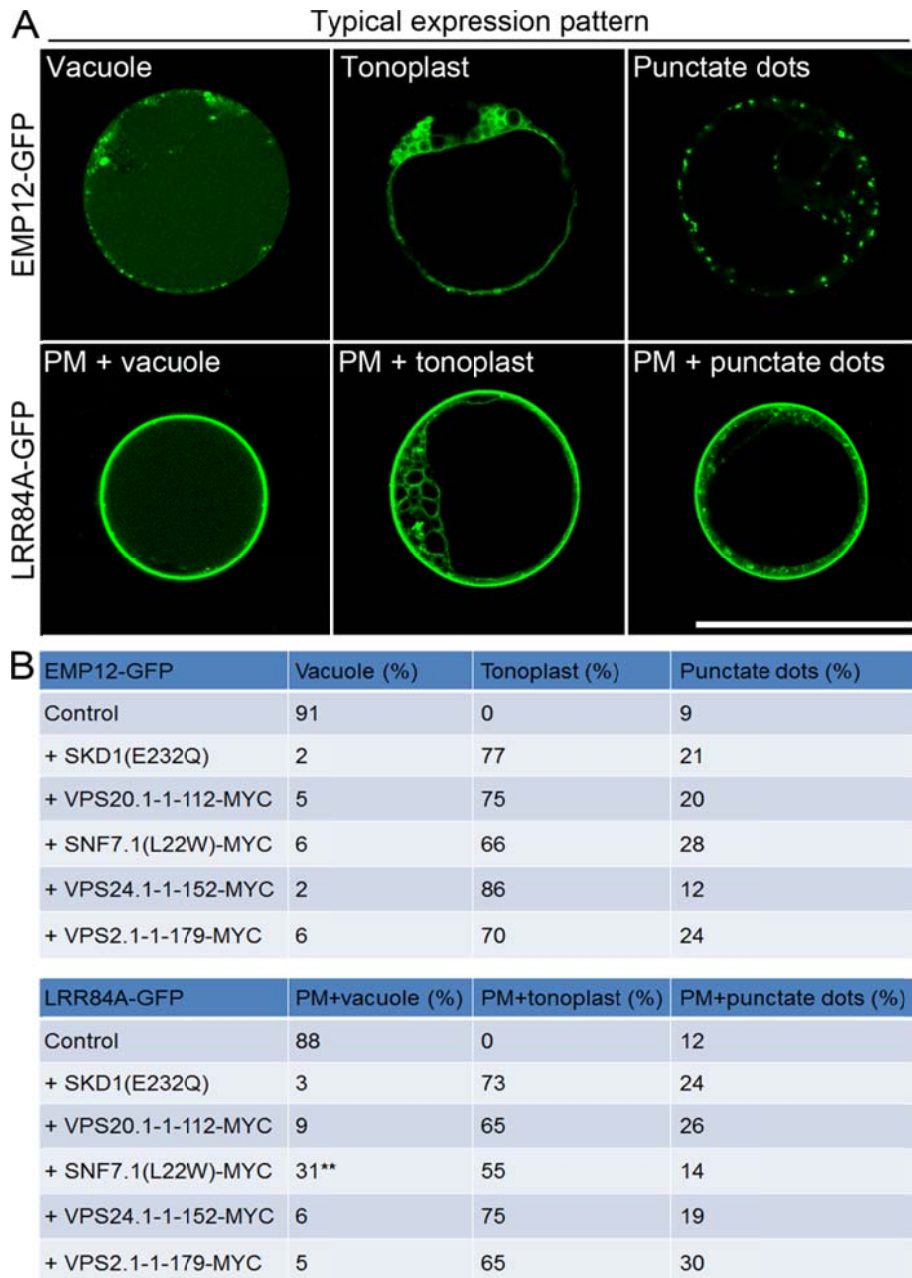
and RFP-VSR2 in *Arabidopsis* protoplasts. Scale bar = 50  $\mu\text{m}$ .



**Supplemental Figure S7.** Coexpression of ESCRT-III subunits did not change the expression pattern of the reporters on the enlarged PVC/MVB. A, Schematic model showing the effect of ESCRT-III coexpression on the localization of the reporters on the enlarged PVC/MVB. B, Coexpression of ESCRT-III dominant negative mutants



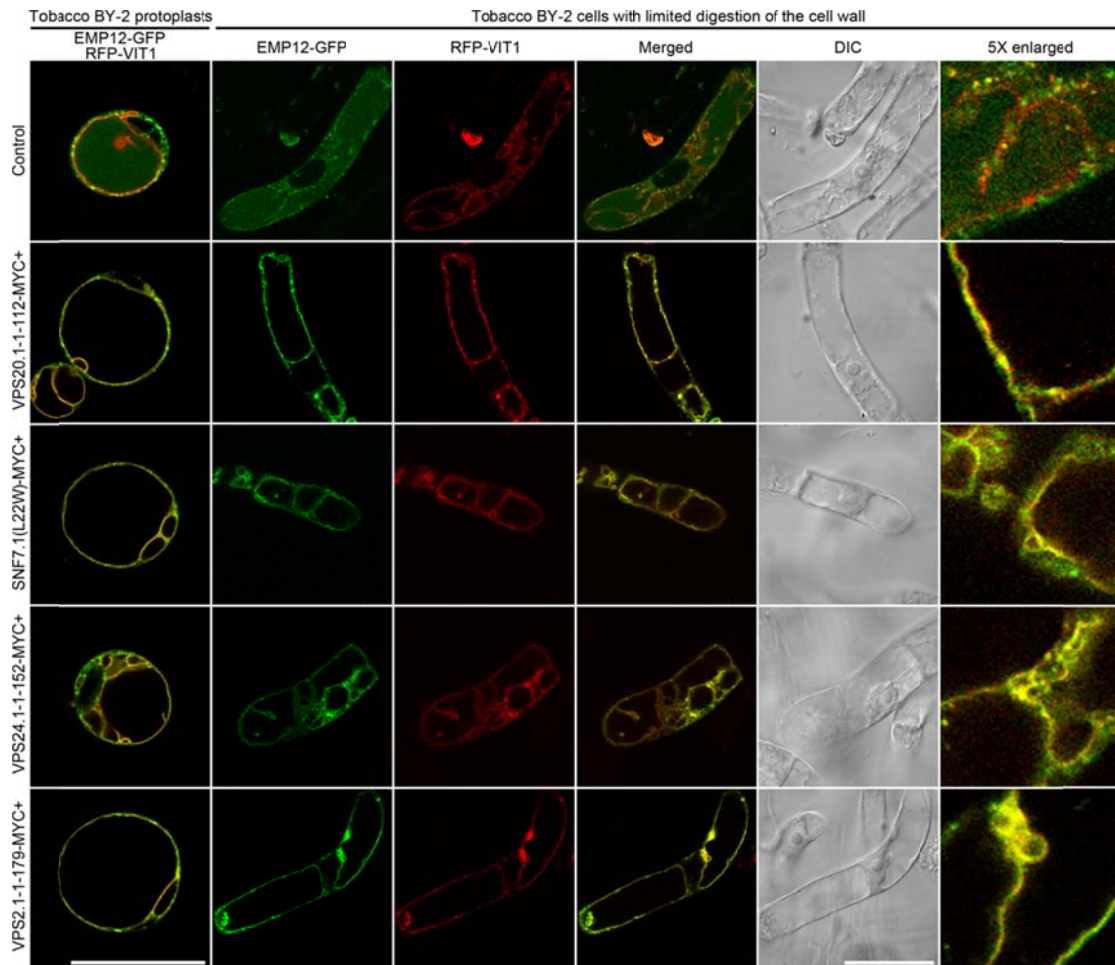
with four reporters and RFP-ARA7(Q69L) in *Arabidopsis* protoplasts. Scale bar = 50  $\mu\text{m}$ .



**Supplemental Figure S8.** Statistic analysis on the expression pattern of protoplasts coexpressing ESCRT-III dominant negative mutants with EMP12-GFP or LRR84A-GFP. ESCRT-III mutants were transiently coexpressed with EMP12-GFP or LRR84A-GFP in *Arabidopsis* PSBD cells.

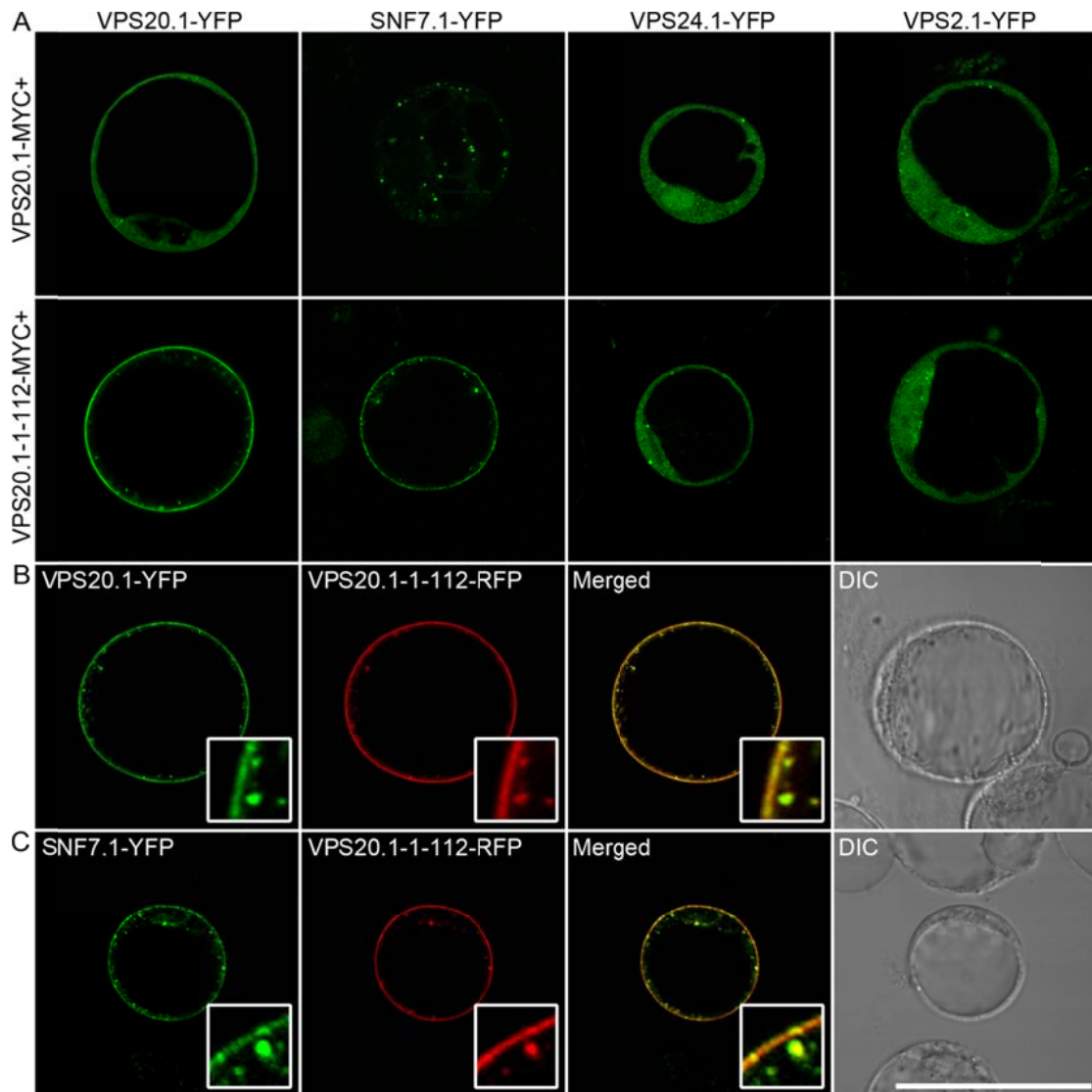
Representative images of different expression patterns were shown (A). Over 100 protoplasts were quantified for each coexpression experiment and statistic analysis data was presented as a percentage of protoplasts displaying each pattern (B). We noted that around 31% protoplasts displayed vacuole pattern in LRR84A-GFP and SNF7.1(L22W)-MYC coexpression experiments as indicated by double asterisk.

However, among these 31% protoplasts, half of them displayed dual localization on the tonoplast. Scale bar = 50  $\mu\text{m}$ .



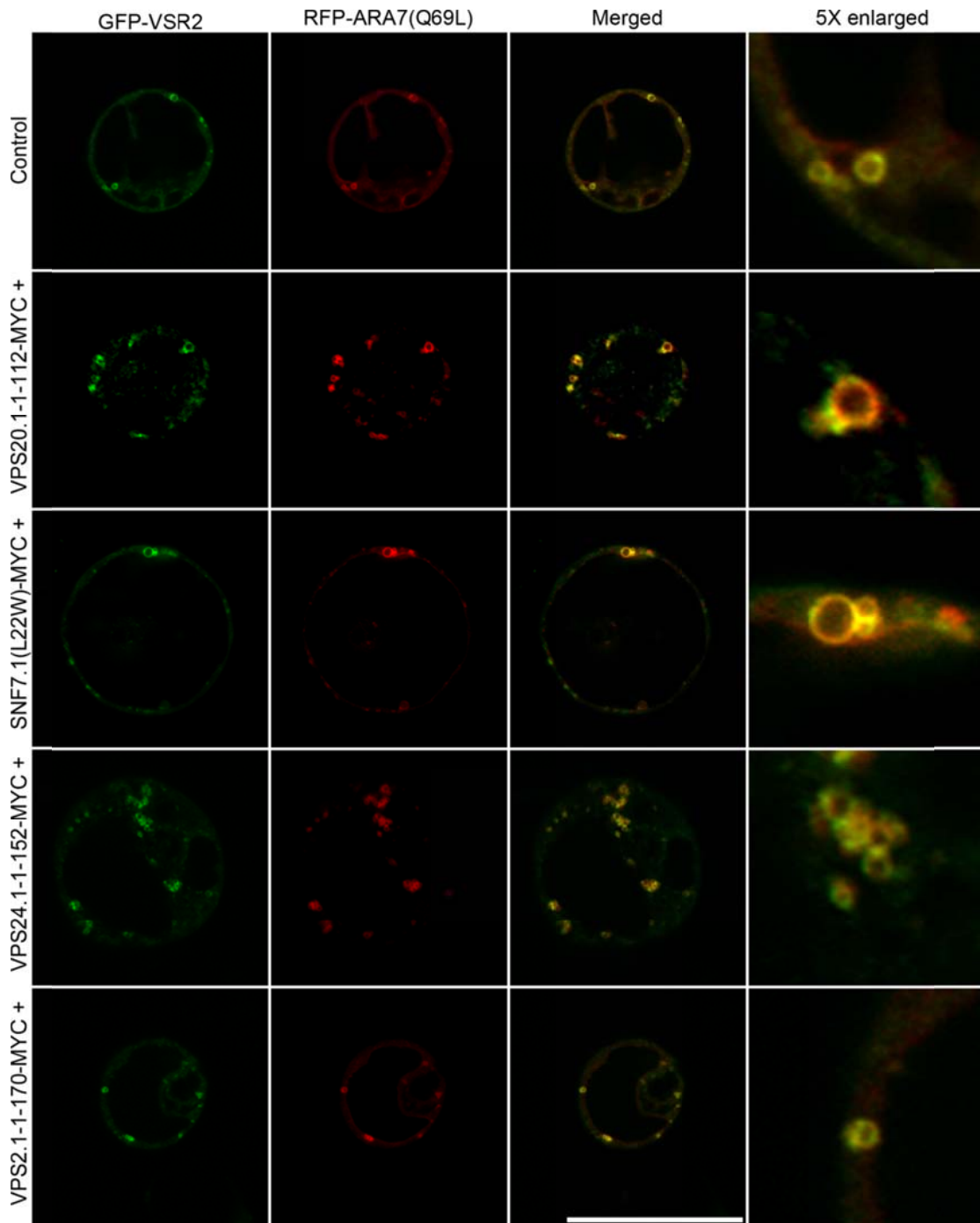
**Supplemental Figure S9.** Coexpression of *Arabidopsis* ESCRT-III dominant negative mutants altered the expression pattern of EMP12-GFP in tobacco BY-2 cells.

*Arabidopsis* ESCRT-III mutants were transiently coexpressed with EMP12-GFP and RFP-VIT1 in tobacco BY-2 protoplasts or tobacco BY-2 cells with limited digestion of the cell wall by cellulicine for 45 minutes to loosen the cell wall. Scale bar = 50  $\mu$ m.

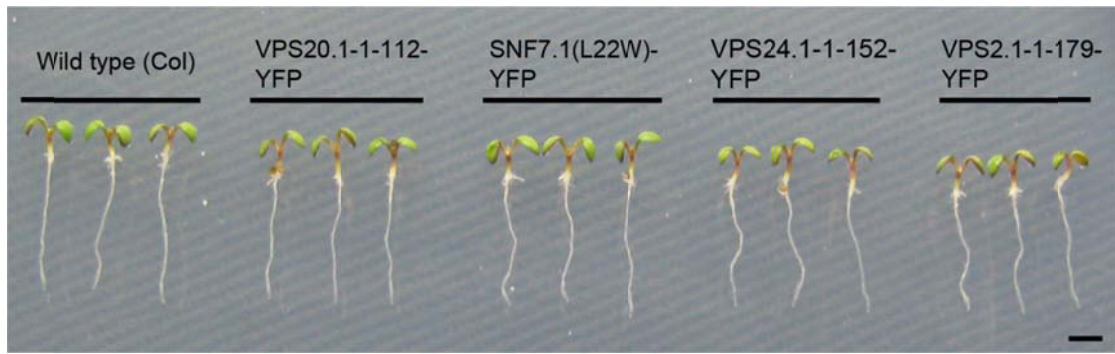


**Supplemental Figure S10.** Effect of VPS20.1-1-112 overexpression on the localization of the ESCRT-III subunits.

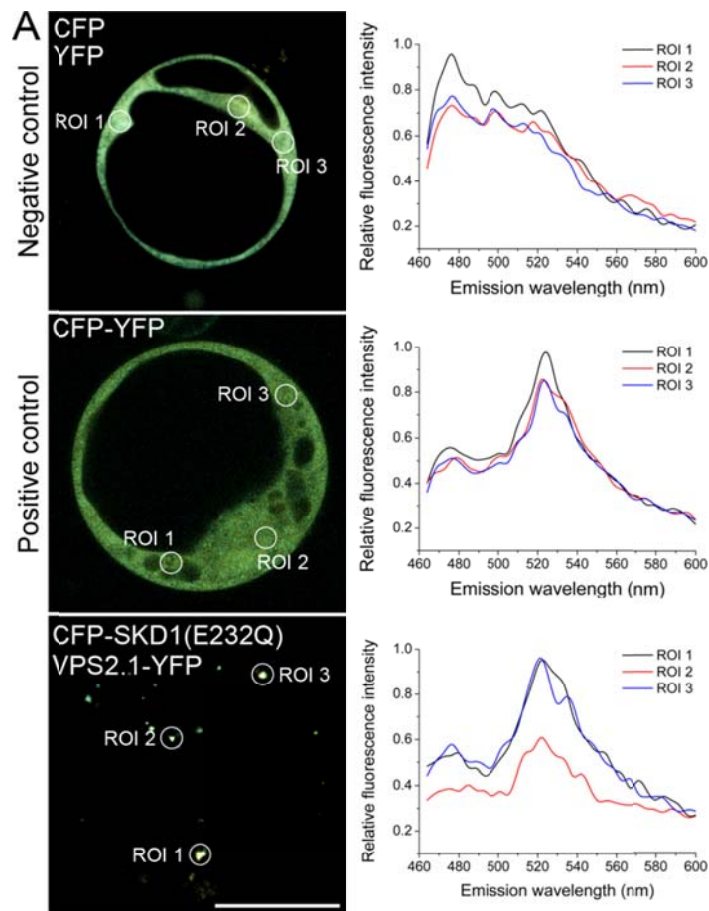
A, ESCRT-III YFP fusions were coexpressed with VPS20.1-MYC or VPS20.1-1-112-MYC in Arabidopsis protoplasts. B and C, VPS20.1-YFP or SNF7.1-YFP was coexpressed with VPS20.1-1-112-RFP in Arabidopsis protoplasts. Scale bar = 50  $\mu$ m.



**Supplemental Figure S11.** Coexpression of ESCRT-III mutants with GFP-VSR2 and RFP-ARA7(Q69L). Scale bar = 50  $\mu$ m.



**Supplemental Figure S12.** Wild type or transgenic *Arabidopsis* plants grown on MS plates without inducer. Scale bar = 2 mm.



**B**

	Signal ratio (522nm/476nm)	Interaction?
CFP + YFP (Negative control)	0.67±0.04	No
CFP-YFP (Positive control)	1.83±0.13	Yes
CFP-SKD1(E232Q) + VPS20.1-YFP	1.52±0.16	Yes
CFP-SKD1(E232Q) + SNF7.1-YFP	1.56±0.26	Yes
CFP-SKD1(E232Q) + VPS24.1-YFP	0.89±0.08	No
CFP-SKD1(E232Q) + VPS2.1-YFP	1.65±0.29	Yes

**Supplemental Figure S13.** SKD1(E232Q) directly interacts with ESCRT-III subunits.

A, Representative images of the negative (CFP coexpressed with YFP) and positive (CFP-YFP tandem fusion expression) controls, and coexpression of CFP-SKD1(E232Q) and VPS2.1-YFP were shown in the left panel. The emission spectrum of three different regions is shown in the right panel. ROI, region of interest. Scale bar = 50  $\mu$ m. B, Quantitative analysis of signal ratios (522nm/476nm) in protoplasts coexpressing CFP-SKD1(E232Q) and different ESCRT-III YFP fusions.